









Aqueous Alteration on Asteroids Simplifies Soluble Organic Matter Mixtures

Junko Isa^{1,2} , François-régis Orthous-Daunay² , Pierre Beck² , Christopher D. K. Herd³ , Veronique Vuitton² , and Laurène Flandinet² 

¹ Earth-Life Science Institute, Tokyo Institute of Technology, Tokyo, Japan; junko.isa@univ-grenoble-alpes.fr

² Université Grenoble Alpes, Grenoble Alpes, CNRS, IPAG, 38000 Grenoble, France

³ Department of Earth and Atmospheric Sciences, University of Alberta, Edmonton, AB, Canada

Received 2021 May 26; revised 2021 September 9; accepted 2021 September 23; published 2021 October 20

Abstract

Biologically relevant abiotic extraterrestrial soluble organic matter (SOM) has been widely investigated to study the origin of life and the chemical evolution of protoplanetary disks. Synthesis of biologically relevant organics, in particular, seems to require aqueous environments in the early solar system. However, SOM in primitive meteorites includes numerous chemical species besides the biologically relevant ones, and the reaction mechanisms that comprehensively explain the complex nature of SOM are unknown. Besides, the initial reactants, which formed before asteroid accretion, were uncharacterized. We examined the mass distribution of SOM extracted from three distinct Tagish Lake meteorite fragments, which exhibit different degrees of aqueous alteration though they originated from a single asteroid. We report that mass distributions of SOM in the primordial fragments are well fit by the Schulz–Zimm (SZ) model for the molecular weight distribution patterns found in chain-growth polymerization experiments. Also, the distribution patterns diverge further from SZ with increasing degrees of aqueous alteration. These observations imply that the complex nature of the primordial SOM (1) was established before severe alteration on the asteroid, (2) possibly existed before parent-body accretion, and (3) later became simplified on the asteroid. Therefore, aqueous reactions on asteroids are not required conditions for cultivating complex SOM. Furthermore, we found that overall H/C ratios of SOM decrease with increasing aqueous alteration, and the estimate of H loss from the SOM is 10%–30%. Organics seem to be a significant H₂ source that may have caused subsequent chemical reactions in the Tagish Lake meteorite parent body.

Unified Astronomy Thesaurus concepts: Carbonaceous chondrites (200); Solar system formation (1530); Molecule formation (2076); Solar nebulae (1508); Protoplanetary disks (1300)

1. Introduction

Abiotic organic compounds are common and widely distributed in solar system objects (Schmitt-Kopplin et al. 2010). Understanding their formation mechanism requires accurate knowledge of their composition at the time of planetesimal accretion, 4.5 Gyr ago, which is complexified by geological processes that occurred on these small bodies over the history of the solar system. In particular, the low-temperature alteration of asteroids, which normally took place a few megayears after accretion at temperatures ranging from $\sim 0^\circ\text{C}$ to $\sim 150^\circ\text{C}$ under aqueous conditions (Suttle et al. 2021), is considered to be an important driver of chemical evolution. This process may have played an essential geological role in producing the building blocks of life, for example, through amplification of L-isovaline excesses (Glavin & Dworkin 2009). A challenge of meteoritic organics studies is to distinguish the preaccretionary (hereafter “primordial”) features from the secondary components that are produced by geological processes on their original asteroidal parent bodies. Inorganic components are distinct across the different chondrite classes and groups; examples include refractory abundances (e.g., Wasson & Kallemeyn 1988), oxidation states (e.g., Urey & Craig 1953), bulk stable-isotope compositions (e.g., Warren 2011), and the size distribution of chondrules (e.g., Jones 2012). On top of the variation of the initial materials, the degree of aqueous alteration and thermal metamorphism can vary for a given meteorite group.

In our study, we examine the Tagish Lake carbonaceous chondrite, an organic-rich (~ 2.5 wt.% organic C), C2 ungrouped meteorite (Grady et al. 2002) that fell on the frozen lake on 2000 January 18 in northwestern British Columbia, Canada. After the

fall, several hundred grams were recovered on January 25 and 26, and the meteorite fragments that had minimum exposure to terrestrial organics are the so-called “pristine” samples. Later, in the spring of 2000, more meteorite fragments were recovered; these are called the “degraded” samples because of terrestrial water contamination (Brown et al. 2000). The pristine collection has provided us a unique opportunity to study abiotic organics and the effects of aqueous alteration on a parent body (e.g., Herd et al. 2011; Gilmour et al. 2019; Simkus et al. 2019). The Tagish Lake meteorite is comprised of several lithologies that experienced different degrees of secondary processing on the same parent body (Zolensky et al. 2002; Herd et al. 2011). We selected three different previously well-studied lithologies: TL5b, TL11h, and TL11i. As a part of the rock, the organics experienced the same geological processes as adjoining inorganic minerals whose textures recorded the degrees of aqueous alteration. Observed trends within the organic matter in Tagish Lake have previously been tied to the degree of aqueous alteration, in the order TL5b (the least altered) < TL11h < TL11i (Herd et al. 2011; Blinova et al. 2014a; Gilmour et al. 2019). The TL5b lithology has the highest abundance of chondrules and lowest abundance of phyllosilicate material; the TL11h and TL11i lithologies have increasing proportions, respectively, of parent-body alteration products, including pore-filling clays (Blinova et al. 2014a). Using thermogravimetric analysis and infrared transmission spectroscopy, Gilmour et al. (2019) showed that these (and other) Tagish Lake lithologies are comparable to the least-altered members of the CM chondrites, equivalent to petrologic types 2.0 (TL5b) through 1.6 (TL11i).

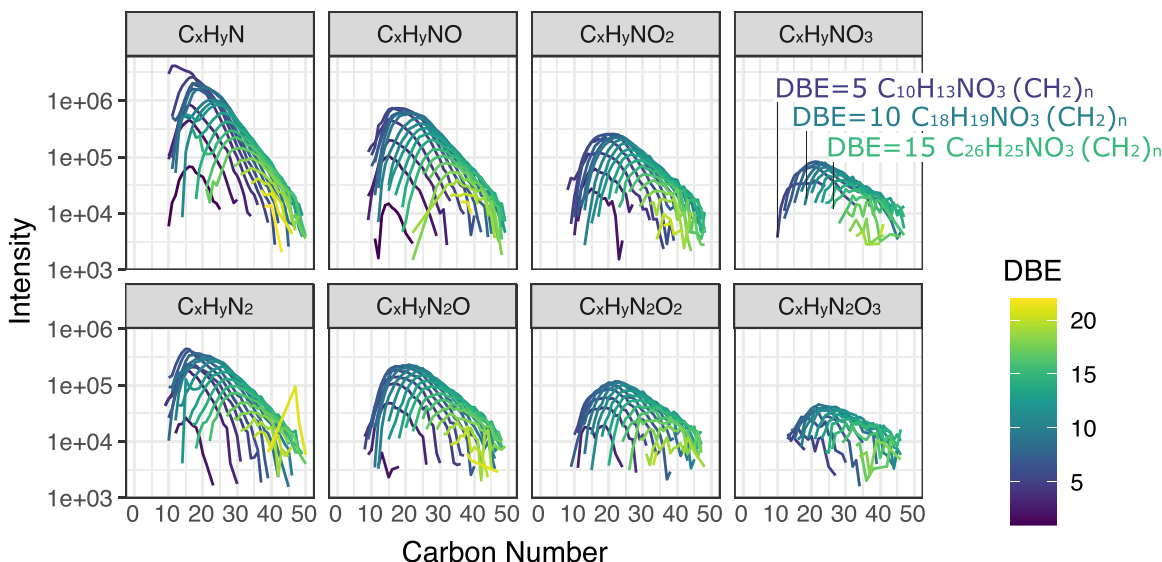


Figure 1. Modified mass spectra as a function of carbon number. The m/z^{-1} that is the mass spectra's x -axis is converted to carbon number. The results are from the least-altered Tagish Lake sample, TL5b. Molecules bearing N(1-3) and O(0-3) were selected, and the data were also organized by the number of heteroatoms, N and O. The completed data can be found in Figure A1. Here DBE denotes the level of unsaturation.

A previous study of insoluble organic matter (IOM) present in Tagish Lake revealed that modification due to the aqueous alteration on the parent body positively and linearly correlates with δD values and H/C ratios, which have been interpreted to reflect the effects of varying degrees of aqueous alteration. For example, the IOM in TL5b (the least altered) has the highest H/C ratios and heavy δD values among the samples from the pristine Tagish Lake collection (Figure 1(b) in Alexander et al. 2014). Thus, one could imagine that the vast majority of soluble organic matter (SOM) was also subject to reactions that led to synthesis or degradation due to their nature to be reactive; indeed, the SOM in Tagish Lake shows similar relationships (Herd et al. 2011; Hilts et al. 2014). Even if the alteration effect does not seem to greatly modify the structure of the macromolecules in the IOM, it may have a dramatic impact on smaller molecules comprising the SOM, either producing them or significantly changing their structure. In particular, the SOM in carbonaceous chondrites is of significant interest, especially the presence of potential biologically relevant compounds such as amino acids, sugars, and fatty acids. In Tagish Lake, the most prominent bulk SOM includes monocarboxylic acids (MCAs) and amino acids that are heterogeneously distributed (Hilts et al. 2014). However, it is still unclear what preaccretionary precursors were present and which formation processes occurred. Thus, it is ambiguous how the organics present in chondrites were formed from those preaccretionary materials. To identify evidence of aqueous alteration of SOM on asteroidal parent bodies, we obtained high-resolution mass spectra of three types of lithologies found in Tagish Lake that experienced different levels of aqueous alteration. We applied a holistic approach to the size distribution of organic molecules. First, we assessed the size diversity of SOM molecular distributions by using the number of heteroatoms and double-bond equivalent (DBE) values ($DBE = C+1-H/2+N/2$) to estimate the level of unsaturation. Second, we fit the data by using a known polymer synthesis model. These data allow one to test previously suggested reaction pathways of organic matter formation in carbonaceous

chondrites, such as a formose-like reaction (e.g., Furukawa et al. 2019).

2. Method

Approximately 10 mg of powdered samples were extracted by using a methanol and toluene (1:2) mixture. The meteorite extract and solvent were separated from the meteorite powder by centrifuging. The direct infusion technique was used with a high-resolution mass spectrometer, the Thermo LTQ Orbitrap XL instrument, coupled with an electrospray ionization (ESI) source in the m/z^{-1} range of 150–800. The positive ions were analyzed with a resolving power of $m/\Delta m \sim 100,000$ at $m/z^{-1} = 400$.

3. Results

We found that the structures in the individual mass spectra from the three extracts from 5b, 11h, and 11i are distinct in terms of their size distributions and relative DBE values. From one sample to another, the molecular size distribution narrows as the degree of aqueous alteration increases. The mass spectra of TL5b can be split into several subspectra in which the DBE and the number of O and N atoms are invariant for the sake of clarity. The shape of the envelope of these subspectra, plotted in Figure 1, appears to be similar regardless of the number of heteroatoms or DBE value. The completed data can be found in Figures A1, A2, and A3. With CHNO only involved in this study, the subspectra turn out to be individual CH_2 families, and they are indeed well fit by the Schulz–Zimm (SZ) distribution that models the molecular weight distribution of chain-growth polymerization experiments (Scholz 1939; Zimm 1948); see Figure 2. Overall goodness of fit (R^2) for the individual CH_2 family (number of family members >10) is shown in Figure 2(d). Notably, the distribution pattern becomes asymmetric and sharp with an increasing degree of aqueous alteration, and the most intense peak of a CH_2 family decreases in mass with an increasing degree of aqueous alteration. These deviations from the SZ distribution seen in the mass spectra are associated with the degree of aqueous alteration. The spikes

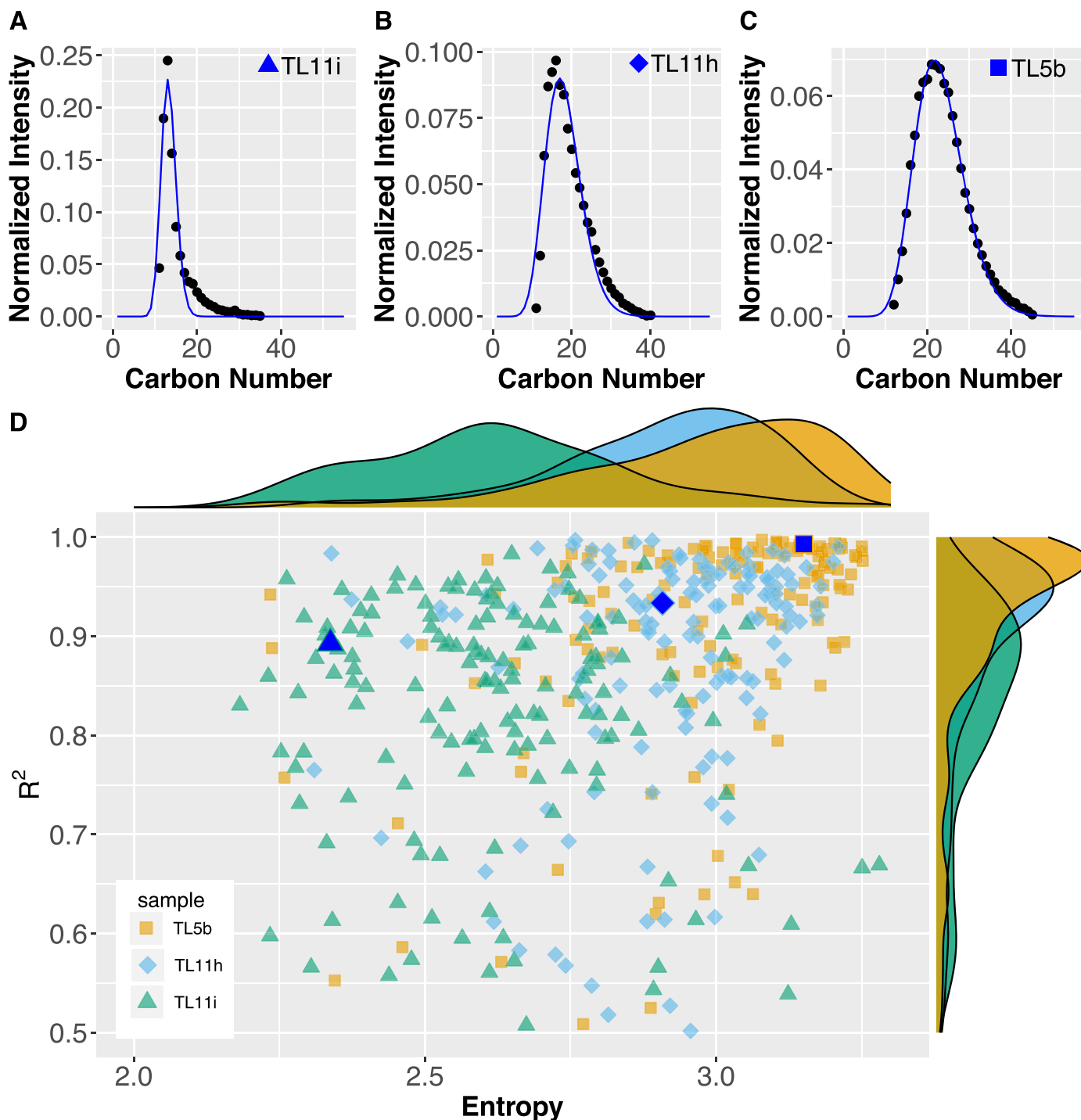


Figure 2. Diversity in size and SZ fit for the data. An example CH_2 family, $\text{C}_{14}\text{H}_9\text{NO} + (\text{CH}_2)_n$, is selected (panels (a)–(c)). The three panels show data from Orbitrap analyses that are arranged in order by the degree of aqueous alteration ($11i > 11h > 5b$). Panel (c) corresponds to the same data in Figure 1 that are presented in the first row ($N = 1$) of the second column ($O = 1$) with the green line for DBE equal to 11. The blue curve in panels (a)–(c) is a fit to the data found via least-squares fitting using an SZ distribution. The curve that can be inferred from the empirical data increasingly diverges from the SZ curves with an increasing degree of alteration. The total amount of detected organic compounds in the three extracted solutions is approximately $11i$ and $11h > 5b$ by the relative intensity against the strong background peak. Thus, the degradations from the model that we see along with the degree of aqueous alteration are not due to the low concentration of SOM in the analyzed solution. Panel (d) is calculated entropy vs. goodness of fit to the SZ distribution of an individual CH_2 family. Although it would be straightforward to plot the shape of all individual spectra (e.g., panels (a)–(c)), we calculated Shannon’s diversity index, aka entropy, $H_{\text{CH}_2 \text{ family}} = -\sum P_i \ln P_i$. The i is the number of carbon atoms in a CH_2 family (e.g., x -axis of panels (a)–(c)) and P_i is probability: normalized intensity for a given number of carbons in a CH_2 family (e.g., y -axis of panels (a)–(c)). The individual density diagrams at the top and right side of the figure indicate frequency density diagrams of the entropy and the goodness of the fit, respectively. The blue filled triangle, diamond, and square correspond to a CH_2 family, $\text{C}_{14}\text{H}_9\text{NO} + (\text{CH}_2)_n$, shown in panels (a), (b), and (c), respectively.

and tailing departing from an SZ distribution indicates that the size diversity is reduced in a CH_2 family, as shown by entropy values calculated for a given CH_2 family (Figure 2(d)).

The results indicate that the hydrogen content in the compounds decreases in more altered samples. While the SOM mass range among the samples is unchanged, the

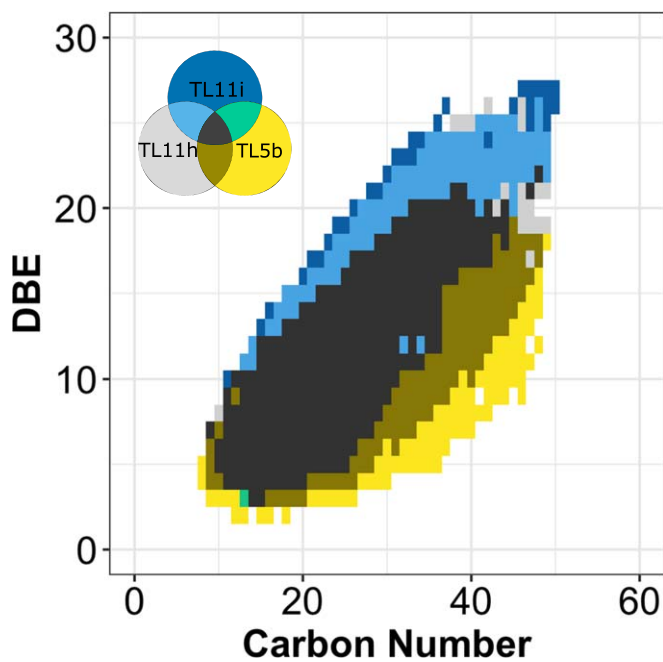


Figure 3. Compare/contrast diagram for the chemical formulae. One O- and two N-bearing formulae were selected (the completed data set can be found in Figure A4). One pixel indicates one chemical formula. The data were color-coded by samples (see Venn diagram). The least-altered samples tend to be plotted at the bottom of the point clouds in the individual boxes (yellow). The most-altered samples tend to be plotted at the top of the point clouds in the individual boxes (blue). This trend indicates that the compounds became oxidized and are either becoming more cyclic or forming double bonds by losing H from the molecules.

maximum DBE increases (Figure 3). The complete data set can be found in Figure A4. The same figure shows that the least-altered sample is the only one that has heavy molecules with low DBE (yellow). The altered samples systematically populate the highest DBE domains (blue). This trend indicates that the carbon atoms in these compounds became oxidized. This trend is also observed in the chemical formulae that are common among the three spectra (black in Figure 3). Normalized intensities among the three samples indicate that the larger DBE intensity increases with a higher degree of alteration given an equal number of carbon atoms in the formulae. Furthermore, we can see that the relatively small molecule intensities are higher in the most-altered sample for the same CH_2 family in Figure A5.

4. Discussion

It is shown in Figure 1 that a high degree of similarity exists in terms of pattern regardless of the number of N or O atoms in the chemical formulae. The least-altered sample is the one where the SZ model explains the observations the best for each individual family and with the best repeatability among the sample family set. These qualities make the SZ model a good candidate to interpret the growth mechanism responsible for the CH_2 variability observed in the mass spectrum. The applicability of the SZ model to different families is remarkable because these patterns and their stability are unlikely to result from reactions caused by a particular functional group (i.e., heteroatoms). It is natural to assume that heteroatoms, which can polarize molecules, should have played a significant role if polymerization occurred in an aqueous fluid in the presence of inorganic ions on the parent body. Therefore, if CH_2 chains

grew during aqueous alteration, one would expect distinct CH_2 polymerization patterns depending on the type and number of heteroatoms. On the contrary, the ubiquity of the SZ patterns tends to show that the complex organic mixture has been synthesized by homogeneous reactions allowing a high degree of branching carbon chains (Pladis & Kiparissides 1998).

The presence of the SZ pattern provides insights into the formation pathways of the organic compounds in the least-altered Tagish Lake sample. Many chemical reaction pathways invoked in previous studies to explain chondrite organics cannot explain the SZ pattern found in the primordial CH_2 polymerization. In particular, condensation reactions in aqueous environments on the parent body that have been proposed to account for IOM-like residues (Cody et al. 2011) or alkylated homologues of N-bearing cyclic compounds (Naraoka et al. 2017) are not capable of explaining the observed SOM distribution. In general, step-growth polymerization involves reactions between two functional groups provided by the monomers and generate a molecular weight variability well described by the so-called Anderson–Flory–Schultz distributions (Försch et al. 2015; see the best fit Figure A6). Such distributions can be found in Fischer–Tropsch-type synthesized mixtures and abiotic RNA polymerization (Spaeth & Hargrave 2020), etc. Therefore, the step-growth hypothesis can be rejected in favor of chain-growth polymerization to explain the CH_2 family groups observed in the least-altered sample.

For the altered samples where a significant deviation from the SZ distribution is found, two hypotheses can be invoked to explain the difference with more primordial samples. One may argue that their occurrence in the most-altered part of Tagish Lake is fortuitous, and they are simply a mixture of several homologous series from primordial organic compounds. So one simple polymerization profile cannot describe them. This possibility cannot be strictly ruled out. However, three remarks should be noted. (1) The observed SOM represents the bulk compositions. It is shown that the bulk elemental compositions of the three lithologies are relatively isochemical (Blinova et al. 2014b; Figure A7). Thus, the sample heterogeneity caused by chondrite accretion processes for the inorganic components are likely less pronounced. (2) Although the Tagish Lake meteorite contains foreign clasts, the compositions of the individual specimens TL5b, TL11h, and TL11i appear to be consistent and can thus be described as lithologies (Blinova et al. 2014a). (3) The distortion from an SZ distribution is gradually enhanced with an increasing degree of alteration. Such an inclination is not expected if the trend was caused by a simple mixture of multiple primordial organic components. Indeed, even chromatographic separation would not be able to distinguish molecules resulting from several synthesis processes in the case where they are identical.

The alternative, which is favored here according to Occam’s razor, is that secondary processes modified an initial synthesis pattern. Although TL5b is the least-altered sample, it is an altered rock (petrologically classified as type 2). Therefore, it is not surprising to see evidence of alteration effects on SOM in our result. A previous study located amorphous silicates in the lithology TL5b matrix, which was interpreted to infer a relatively low alteration temperature of $\leq 50^\circ\text{C}$ (Blinova et al. 2014a). We can recognize these mild alteration effects in our measured SOM distribution. Although most CH_2 families in the least-altered sample, TL5b, maintained their SZ profile throughout the alteration, as depicted by data points with higher entropy and R^2 values close to 1 (Figure 2(d)), some distortions

from the SZ profile are found in a few CH₂ families. That alteration evidence is depicted as the yellow data points with lower entropy and smaller R^2 values (Figure 2(d)). Therefore, the SZ pattern extrapolated from the three samples can be taken as representative of the original soluble organic makeup that was perhaps established before accretion of the Tagish Lake parent body. The possible chemical reaction field to establish the SZ profile is not limited to aqueous conditions or low temperature. For example, the polymers can be synthesized from gas by chain-growth reactions (Alves et al. 2021). And high-temperature gas-phase experiments can form various organics ranging from IOM-like material to small molecules comparable to SOM, as well as the production of the xenon mass fraction observed in the matrix known as the Q-phase (Kuga et al. 2015, 2017; Bekaert et al. 2018). The SOM mass distributions of those materials can indeed be well fit by the SZ model (Figure A8). We show the distributions and SZ fit in a figure together with the data (Figure A9). These high-temperature reactions provide an interesting pathway to form SOM. High-temperature conditions can be found in the irradiated parts of the solar nebula. Extraterrestrial samples also record massive high-temperature processing of protoplanetary disk materials by the widespread occurrence of chondrules. These formed under high-temperature and high ambient gas pressure transient events (by evaporating the gas during their formation) in the solar nebula (Alexander & Ebel 2012 and references therein). We do not rule out the possibility of the formation mechanisms besides in a vapor phase. And yet, forming the SZ profile of the SOM complex before accretion is plausible and consistent with the rest of the chondrite components.

Aqueous alteration processes resulted in an oxidized signature (that is, the loss of H) of the SOM, which is consistent with the previously observed linear correlation in the H/C ratios and δD of Tagish Lake IOM (Cody & Alexander 2005; Alexander et al. 2007; Herd et al. 2011; Alexander et al. 2014) and inferences from previous IOM and SOM studies (Hilts et al. 2014; Quirico et al. 2018). The present measurement shows that the larger molecules were spared from removal throughout the alteration (Figure 3), as depicted in the point clouds. A chemical change is observed in the composition of the individual molecules: the most-altered samples shift toward higher DBE. Such hydrogen elimination reactions can take place by adding energy to a system. The H loss from organics was confirmed after heating meteorite IOM (Yabuta et al. 2007; Oba & Naraoka 2009) and after irradiating meteorite SOM (Orthous-Daunay et al. 2019). In the reactions that occurred during aqueous alteration, the processes were likely facilitated by heating of the parent asteroids. It is likely that such raised temperature conditions caused the same reaction mechanisms that resulted in hydrogen loss in both IOM and SOM. This hypothesis can be tested by comparing the degree of H loss between IOM and SOM. The averaged H/C ratios of SOM and IOM decrease with increasing alteration degree, TL11i (the most altered) < TL11h < TL5b (the least altered). By using TL5b as a reference, we semiquantitatively estimated the H loss in TL11h and TL11i SOM. The estimated H loss from SOM was approximately 10%–30%, while that from IOM it was 18% and 30% for TL11h and TL11i, respectively (Figure A10). In addition, this consistent H loss caused by alteration in both SOM and IOM indicates that the primordial organic compounds matured during the alteration

regardless of their size. As a consequence of oxidation in both SOM and IOM, the organics released hydrogen to the environment, likely affecting subsequent chemical reactions on the asteroids. Hydrogen is also known to be produced by metal oxidation during the aqueous alteration of the chondrite parent bodies. Therefore, at least two distinct mechanisms can be major contributors of H₂ in chondrite parent bodies. The hydrogen degassing has been considered an essential step to explain H-isotope heterogeneities found in chondrite components. Alexander et al. (2010) suggested that the Rayleigh-type fractionation, caused by H₂ degassing, can create D-rich water through the equilibrium between the remaining deuterium-rich H₂ and water. Subsequently, the D-rich water–organic reactions may have produced D-rich organics. Moreover, H₂ in the environment has been considered to react with oxide metals. The H₂ produced from organics could have reacted with surrounding minerals, including dissolved carbonates (Zolotov et al. 2006; Guo & Eiler 2007). Interestingly, the total abundance of carbonate minerals in the three Tagish Lake lithologies also correlates with the degree of aqueous alterations, 8, 5, and 4 vol% for TL5b (the least altered), TL11h, and TL11i (the most altered), respectively (Table A1). Further C-isotope studies in the individual carbonate grains in the three samples may reveal details concerning the organic and inorganic carbon chemistry and the timing relative to the H₂-producing events.

In addition to the loss of hydrogen, the alteration produced an increase in small molecules (shift to low mass in Figure 2 and supplemental figures). Previously observed MCAs in the Tagish Lake meteorite are abundant, 100 ppm for bulk rock (Pizzarello et al. 2001). The minimum estimates for individual lithologies are 500 ppm for 5b and 11h and 300 ppm for 11i (Hilts et al. 2014). Previous studies showed that the concentration distribution of MCA CH₂ families in the Tagish Lake meteorite changed with increasing alteration (Hilts et al. 2014, Figure 6(b)). The abundance of MCA with a carbon number ranging from 4 to 10 in TL5b became low relative to formic acid (C1) and acetic acid (C2) in TL11i. The diminished diversity in size by alteration is consistent with the overall trend seen in Figure 2. The distribution becomes sharper when compared to the less altered broad spectrum due to a decrease for large carbon number molecules and an increase at small carbon numbers. Thus, our study agrees with the Hilts et al. (2014) results and extends the observations to ~4200–5000 chemical formulae.

Finally, our results can be utilized for assessing the SOM alteration degree in samples that have experienced aqueous alteration on their various chondritic components. For example, Naraoka & Hashiguchi (2019) found that alkylpiperidines are more abundant in Yamato 002540 (CR) than in Murray (CM2), while alkylpyridine concentrations are high in Murray relative to Yamato 002540. By investigating their mass distributions, one can estimate the degree of alterations that took place on their parent bodies. Furthermore, studies of samples such as those from the asteroid missions to Ryugu and Bennu that were brought back by the JAXA Hayabusa2 and or will be brought back the NASA OSIRIS-Rex spacecraft, respectively, can be impacted by our findings. These asteroids consist of carbonaceous chondrite material that has undergone parent-body alteration. For example, one can assess the biorelated molecular synthesis found due to parent-body alteration by calculating the

residual from the SZ model for homologous series as used in this study.

5. Conclusion

We studied the mass distribution of SOM extracted from three distinct Tagish Lake meteorite fragments. We found that (1) the mass distributions of the SOM found in the primordial fragments can be explained using the SZ model, (2) the mass distribution pattern becomes asymmetric and sharper with increasing degrees of aqueous alteration, and (3) the carbon atoms in these compounds became more oxidized with increasing degrees of aqueous alteration. These observations imply that the complex nature of the primordial SOM (1) was established before severe alteration on the asteroid and that mechanisms accounting for the alteration can be explained by chain-growth polymerization, (2) was possibly established in the solar nebula, (3) was simplified on the asteroid, and 4) matured together with IOM. Therefore, it appears that the reaction pathways that have been suggested for explaining complex SOM on asteroids are not necessarily correct, since the complexities seem to be preexisting even though aqueous reactions were necessary to synthesize specific biotically relevant compounds, such as amino acids (Koga et al. 2021), ribose (Furukawa et al. 2019), or RNA (Cafferty & Hud 2014). Furthermore, one can identify which organic chemical formulae were preferentially synthesized through metamorphism and alteration on asteroids relative to other solar nebula materials by measuring deviations from the SZ model.

We thank Dr. Lee Frost Bargatze for constructive criticism of the manuscript. This work is supported by the French National Research Agency in the framework of the Investissements d’Avenir program (ANR-15-IDEX-02) through the funding of the “Origin of Life” project of the Univ. Grenoble Alpes. P.B. acknowledges funding from the European Research Council under the H2020 framework program/ERC grant agreement No. 771691 (Solarys).

Appendix A Supplement Figures and a Table

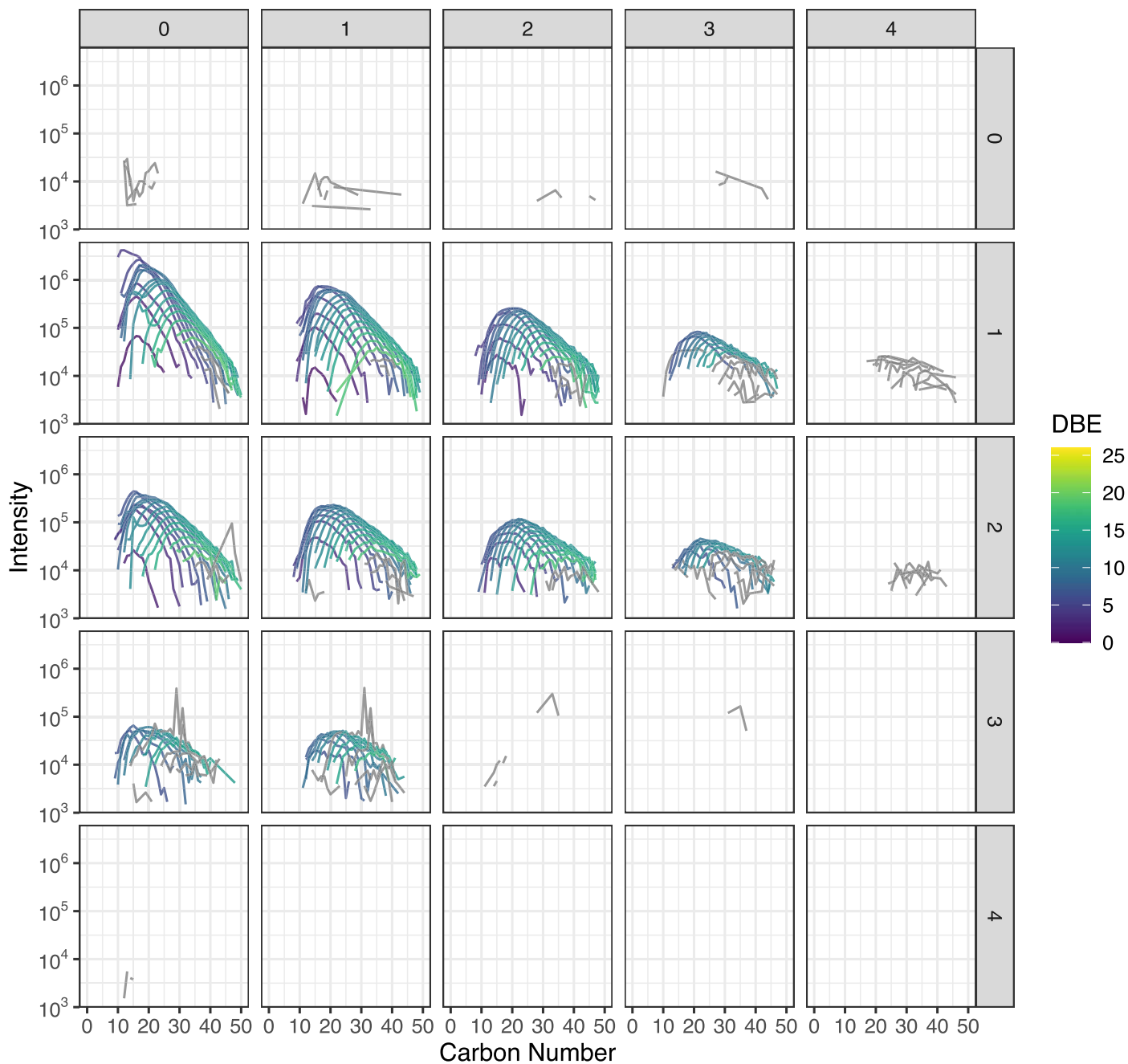
In Figure 1, we present the selected modified mass spectra as a function of carbon number based on the results of the least-

altered Tagish Lake sample, TL5b. In Figures A1–A3, we show the completed data set. In Figure 3, we present the selected compare/contrast diagram, which data are selected only one O- and two N-bearing formulae. In Figure A4, we show the completed data set; in Figure A5, we show the common chemical formulae of samples 5b, 11h, and 11i. In Figure 2 (a-c), we present the diversity in size and Schulz-Zimm (SZ) fit for the data. In Figure A6, we show the same data with the Anderson-Flory-Schultz fit. In Figure A7, we show bulk Zn/Mn ratios of the Tagish Lake meteorite, CM group based on the previously reported data. In Figure A8 and A9, we show modified mass spectra as a function of carbon number based on the results of the Nebulotron material. In Figure A10, we show atom H/C ratio of SOM vs. that of IOM. In the Table A1, we show the bulk rock mineralogy and components of Tagish Lake samples.

Table A1
Bulk Rock Mineralogy and Components of Tagish Lake Samples

	5b wt %	11h wt %	11i wt %
Forsterite	39	15	19
Magnetite	30	18	19
Pyrrhotite	8	8	4
Enstatite	3	n/d	n/d
Dolomite	2	n/d	n/d
Siderite	10	10	7
Calcite	2	0	1
Clinocllore	n/d	48	48
Amorphous	7.6	1.7	2.6
	vol%	vol%	vol%
Chondrules	30	25	5
Magnetite	18	15	15
Sulfides	7	4	2
Isolated silicate	10	1	5
Carbonate	8	5	4
Lithic fragments	2	10	13
Matrix	25	42	54

Note. The data are from Blinova et al. (2014a).



rows = numbers of N atoms and columns = numbers of O atoms

Figure A1. Modified mass spectra as a function of carbon number. The results are from the sample TL5b. We define a CH₂ family, known as an alkyl homologous series, as all molecules that have the same stoichiometric formulae except for the number of repeating CH₂. They are treated similar to the alkyl homologous compounds that were identified in a previous study of the Murchison meteorite (Naraoka et al. 2017). The data were also organized by the number of heteroatoms, N and O, colored by DBE values. The data in gray are filtered out for Figure 2. The filtering criteria are that the number of peaks in a CH₂ family is larger than 10, the calculated entropy is >2 , and the goodness of the SZ fit is >0.5 .

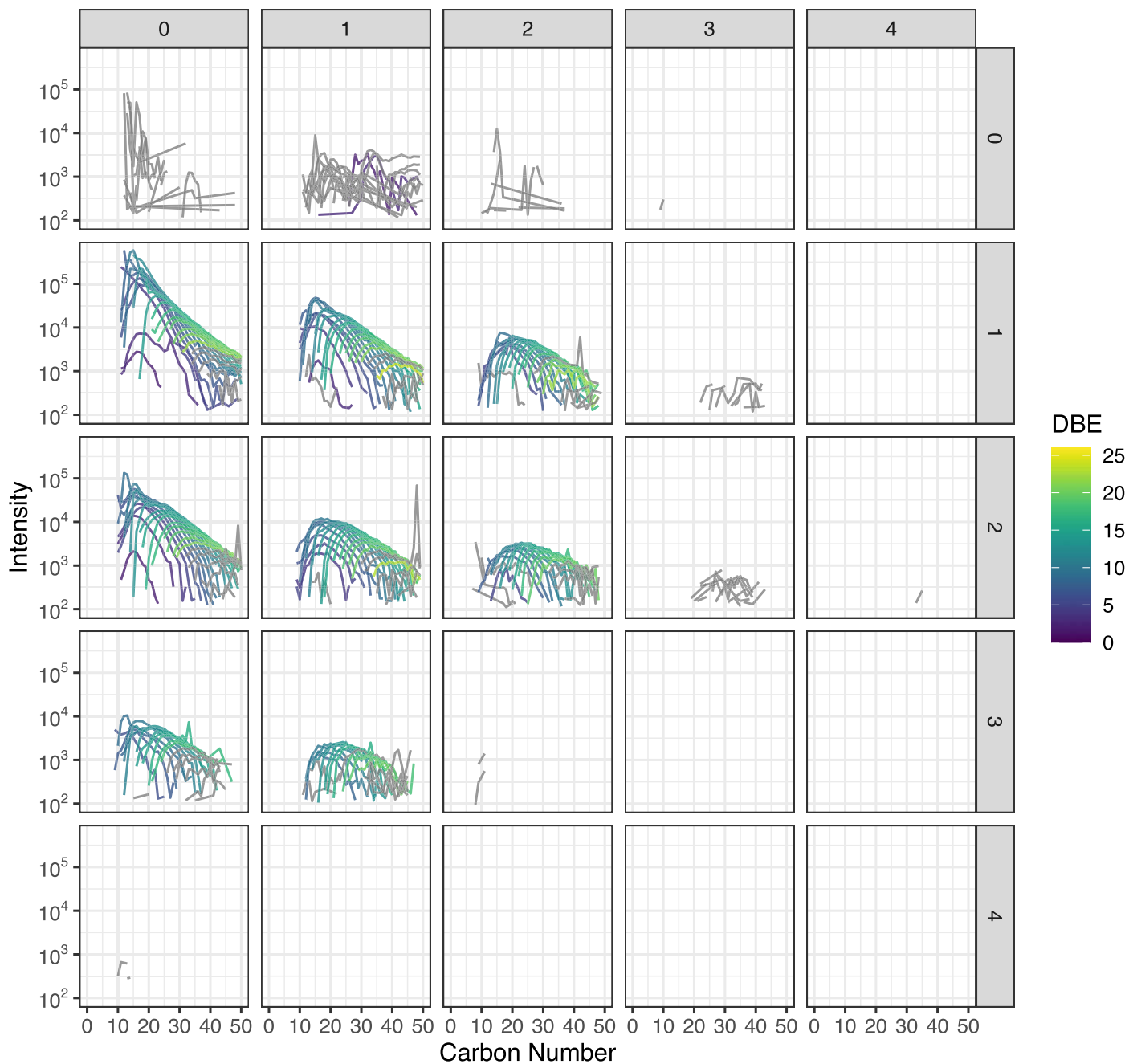


Figure A2. Modified mass spectra as a function of carbon number. The results are from the sample TL11h. We treated the stoichiometric formulae varying in CH_2 as a repeating unit and call them as CH_2 family respect to DBE values after the chemical assignment. They are treated similar to the alkyl homologous compounds that were identified in a previous study of the Murchison meteorite (Naraoka et al. 2017). The data were also organized by the number of heteroatoms, N and O, colored by DBE values. The data in gray are filtered out for Figure 2. The filtering criteria are that the number of peaks in a CH_2 family is larger than 10, the calculated entropy is >2 , and the goodness of the SZ fit is >0.5 .

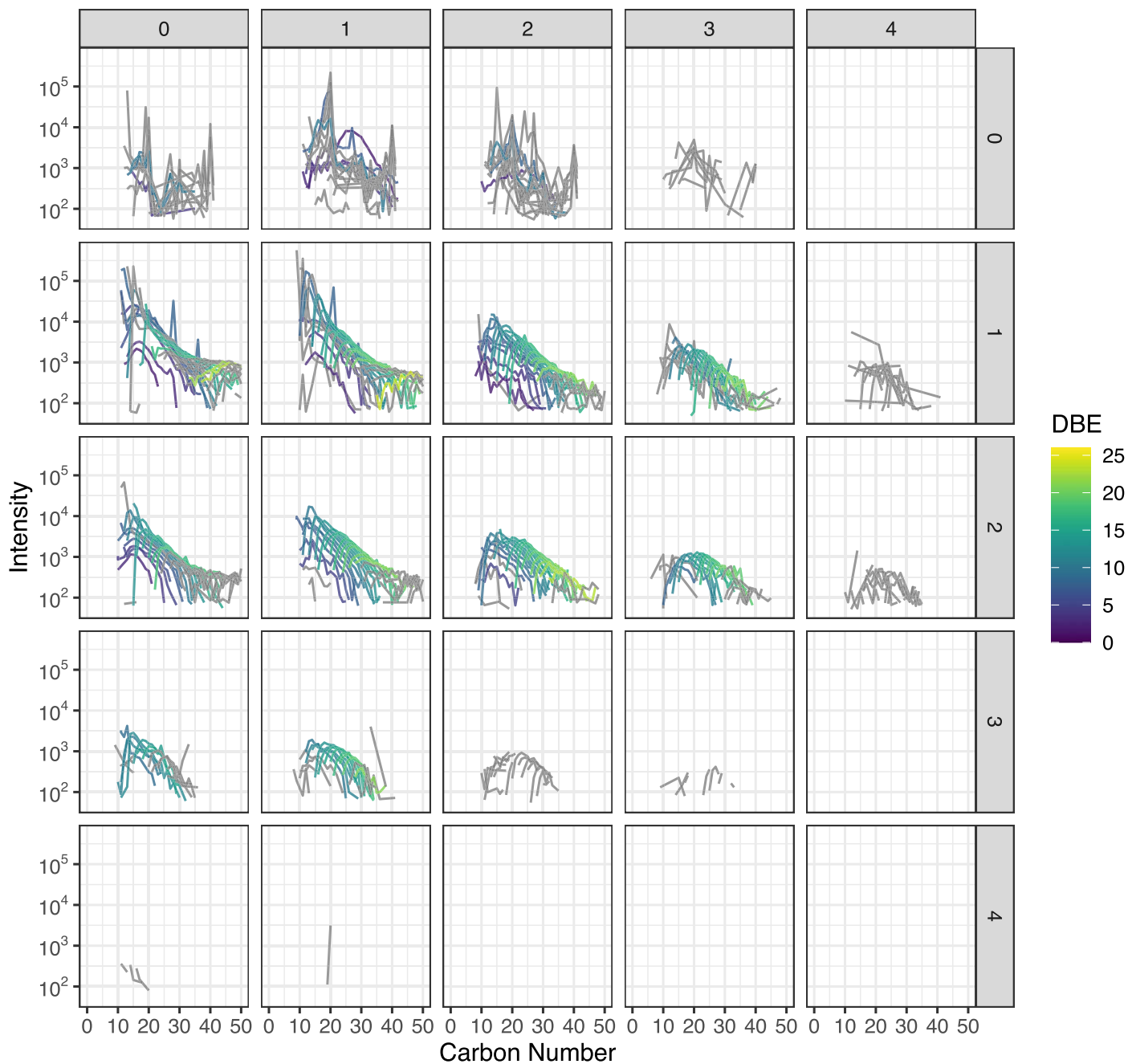


Figure A3. Modified mass spectra as a function of carbon number. The results are from the sample TL11i. We treated the stoichiometric formulae varying in CH_2 as a repeating unit and call them as CH_2 family respect to DBE values after the chemical assignment. They are treated similar to the alkyl homologous compounds that were identified in a previous study of the Murchison meteorite (Naraoka et al. 2017). The data were also organized by the number of heteroatoms, N and O, colored by DBE values. The data in gray are filtered out for Figure 2. The filtering criteria are that the number of peaks in a CH_2 family is larger than 10, the calculated entropy is >2 , and the goodness of the SZ fit is >0.5 .

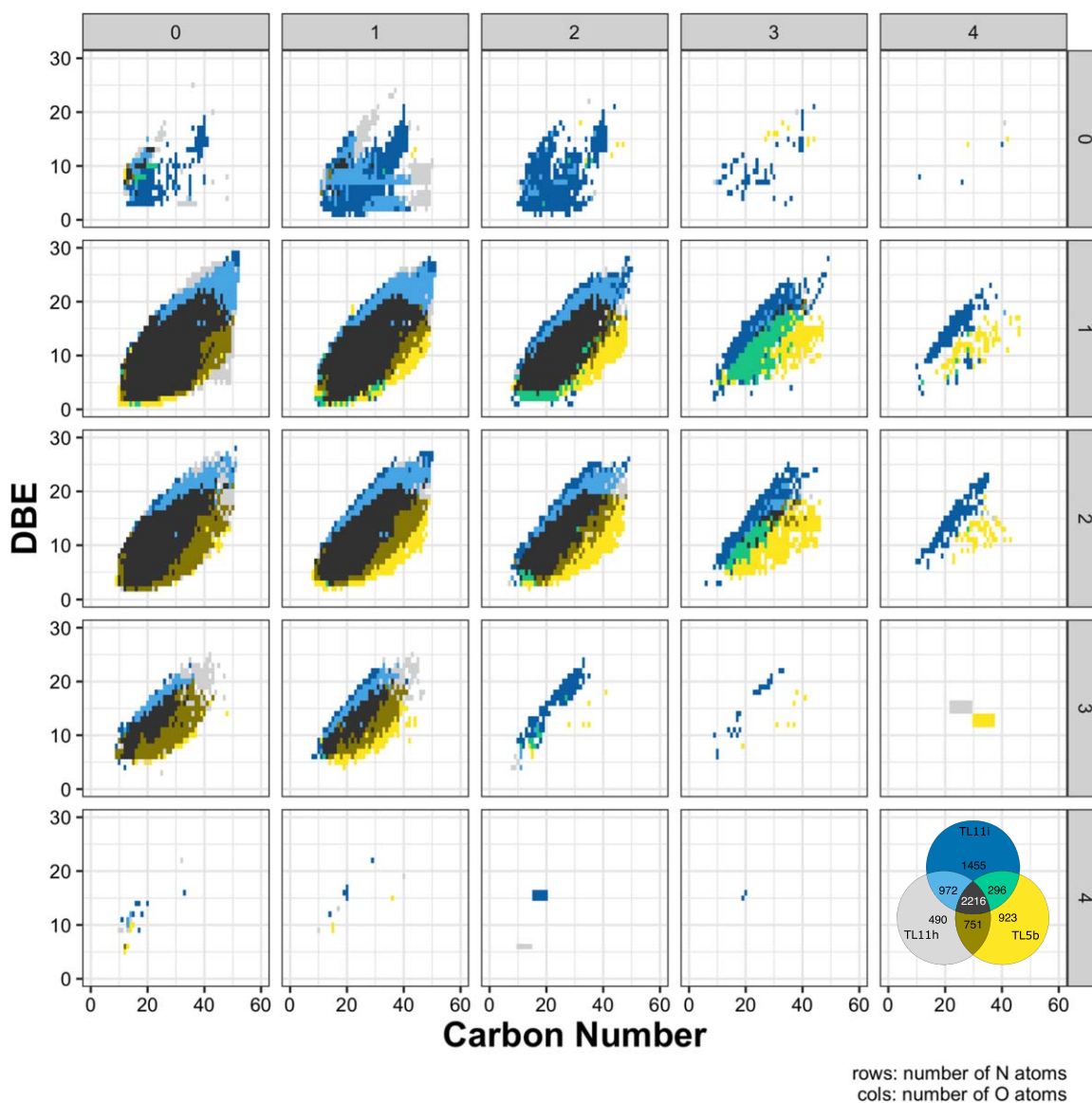


Figure A4. The common and divergence of assigned chemical formulae. The individual boxes are organized by the number of heteroatoms in the chemical formulae. One pixel indicates one chemical formula. The data were color-coded by samples (see Venn diagram). The least-altered samples tend to be plotted at the bottom of the point clouds in the individual boxes (yellow). The altered samples tend to be plotted at the top of the point clouds in the individual boxes (blue). This trend indicates that the compounds became oxidized and are either becoming more cyclic or forming double bonds.

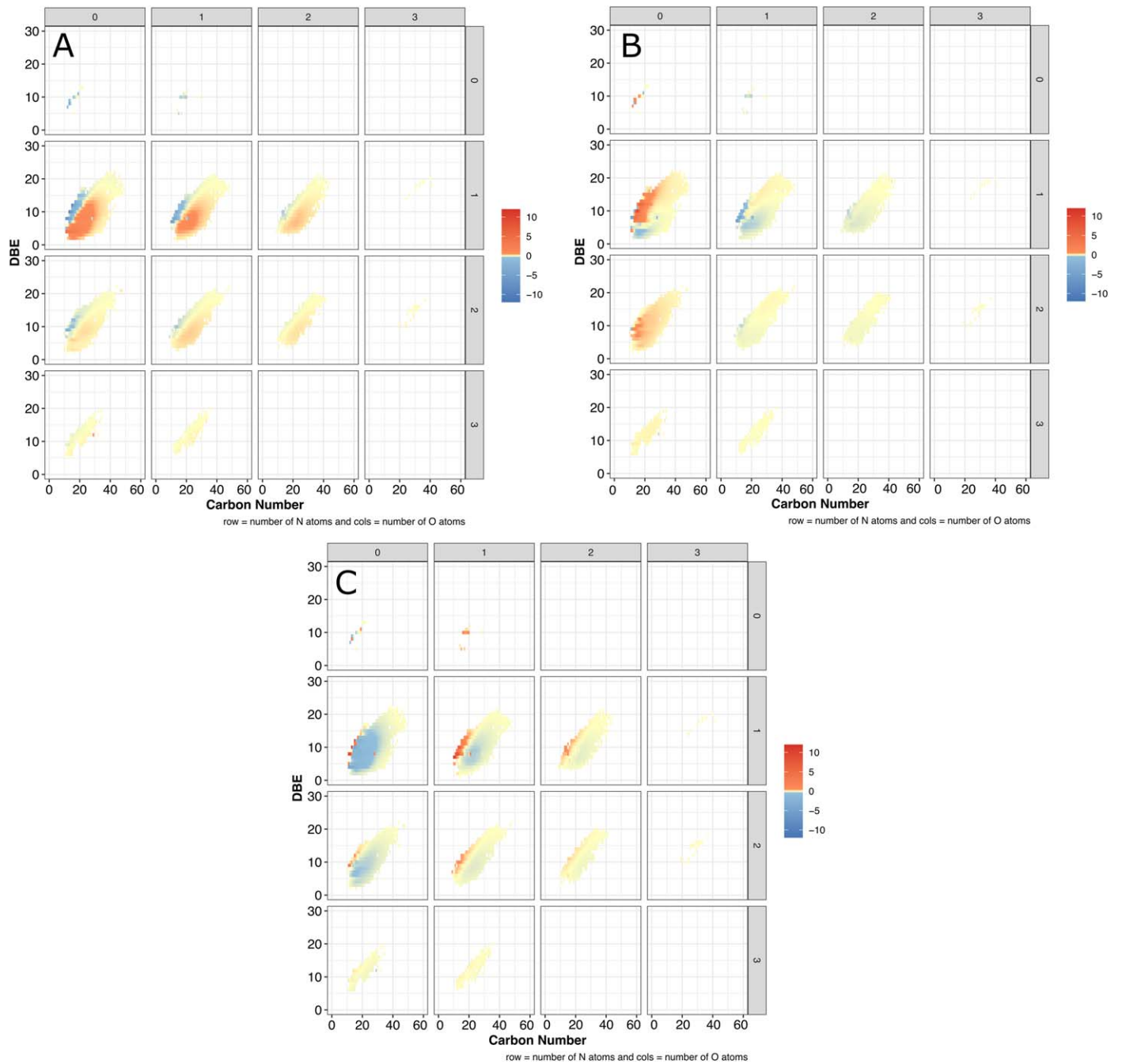


Figure A5. Common chemical formulae of samples 5b, 11h, and 11i (at the center of the Venn diagram; see Figure A4). Shown are the normalized intensities among the three samples. Panels (a), (b), and (c) represent samples 5b, 11h, and 11i, respectively. The positive (red) or negative (blue) index indicates the intensities that are higher or lower than the normalized average intensities. With an increasing degree of alteration, the larger DBE chemical formula intensity increases.

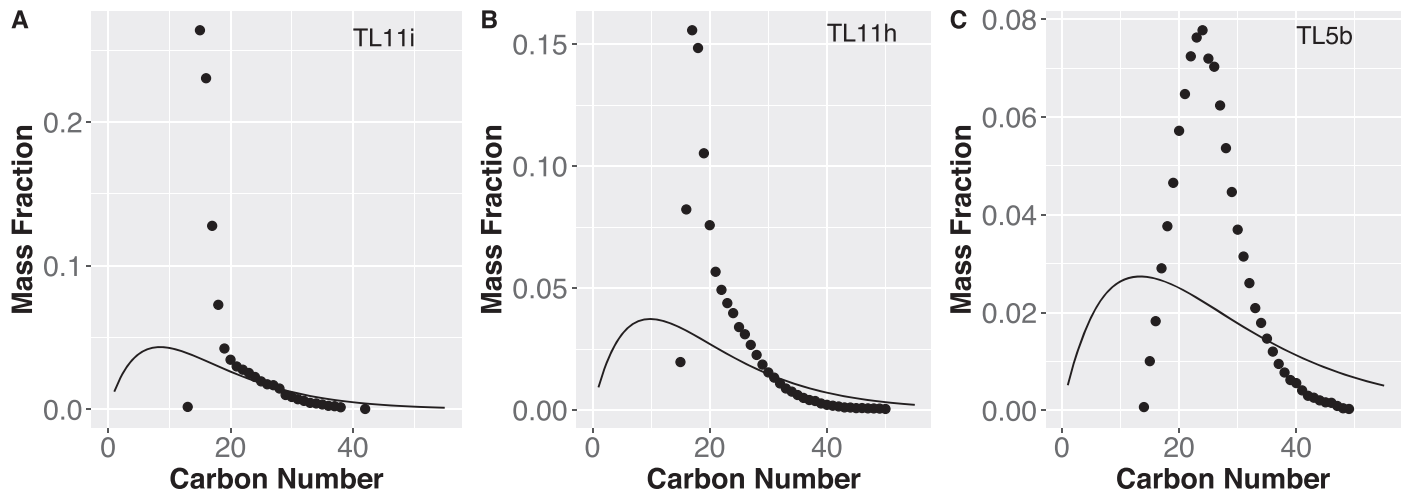


Figure A6. Example CH_2 family, $\text{C}_{14}\text{H}_9\text{NO} + (\text{CH}_2)_n$. The same data are plotted in Figures 2(a)–(c). The black solid line is the best fit of the Anderson–Flory–Schultz distribution to the data set. The data are not well explained by the Anderson–Flory–Schultz model.

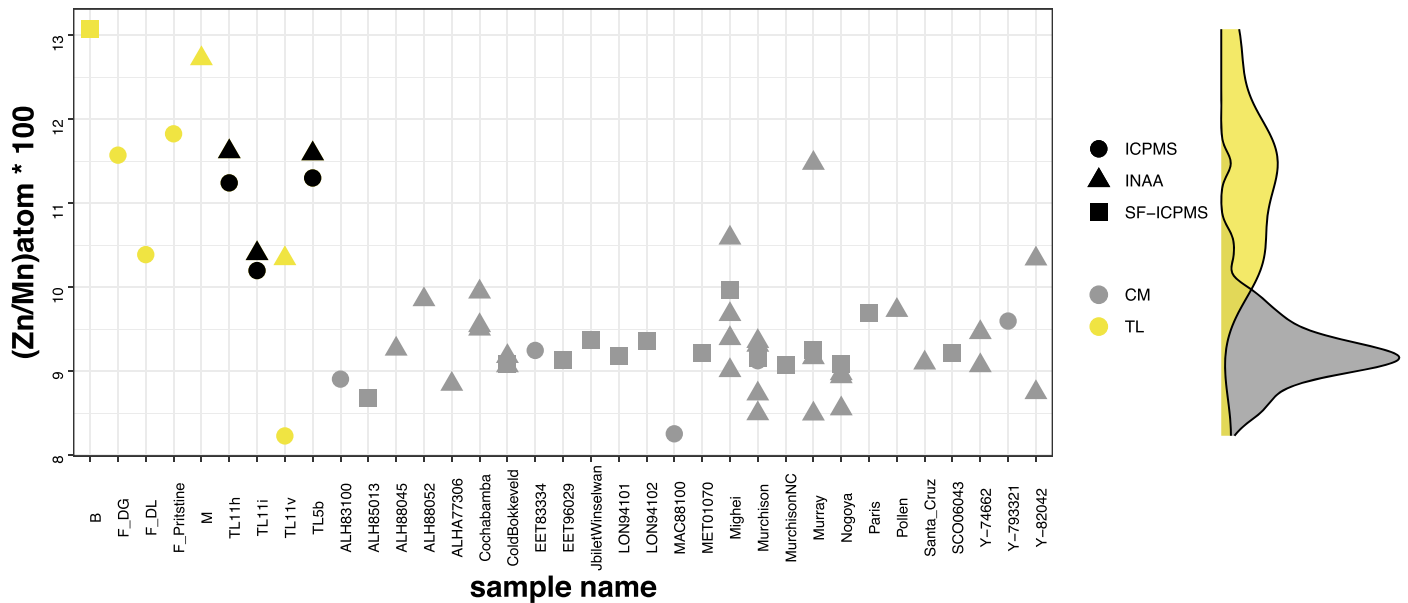


Figure A7. Bulk Zn/Mn ratios of the Tagish Lake meteorite group based on the previously reported data. The ratio of the moderately volatile element, Mn, and volatile element, Zn, is one of the representations of accretionary material diversity. Assuming that the scatter within the CM is an example of a typical variety of chondrite groups, the samples used in this study, TL11h, TL11i, and TL5b (black symbols), are homogeneous, while Tagish Lake lithology TL11v, for example, shows a relatively large heterogeneity. That disagreement in the aliquots can indicate the contamination from the foreign clast that was located in the Tagish Lake meteorite. On the contrary, lithologies TL11h, TL11i, and TL5b are closer to the average Tagish Lake meteorite value. Their duplicate analyses by the different aliquots using the distinct analytical techniques agree well with each other. The Tagish Lake meteorite data includes the following: B (Braukmüller et al. 2018); F_DG (Disturbed_G; Friedrich et al. 2002); F_DL (Disturbed_L; Friedrich et al. 2002); F_Pristine (Pristine; Friedrich et al. 2002); M (Mittlefehldt 2002); and TL11h, TL11i, TL11v, and TL11v (Blinova et al. 2014b). The CM chondrite data are previously reported INAA and ICP-MS data (Kallemeyn & Wasson 1981; Grady et al. 1987; Wlotzka et al. 1989; Mittlefehldt 2002; Friedrich et al. 2002; Braukmüller et al. 2018).

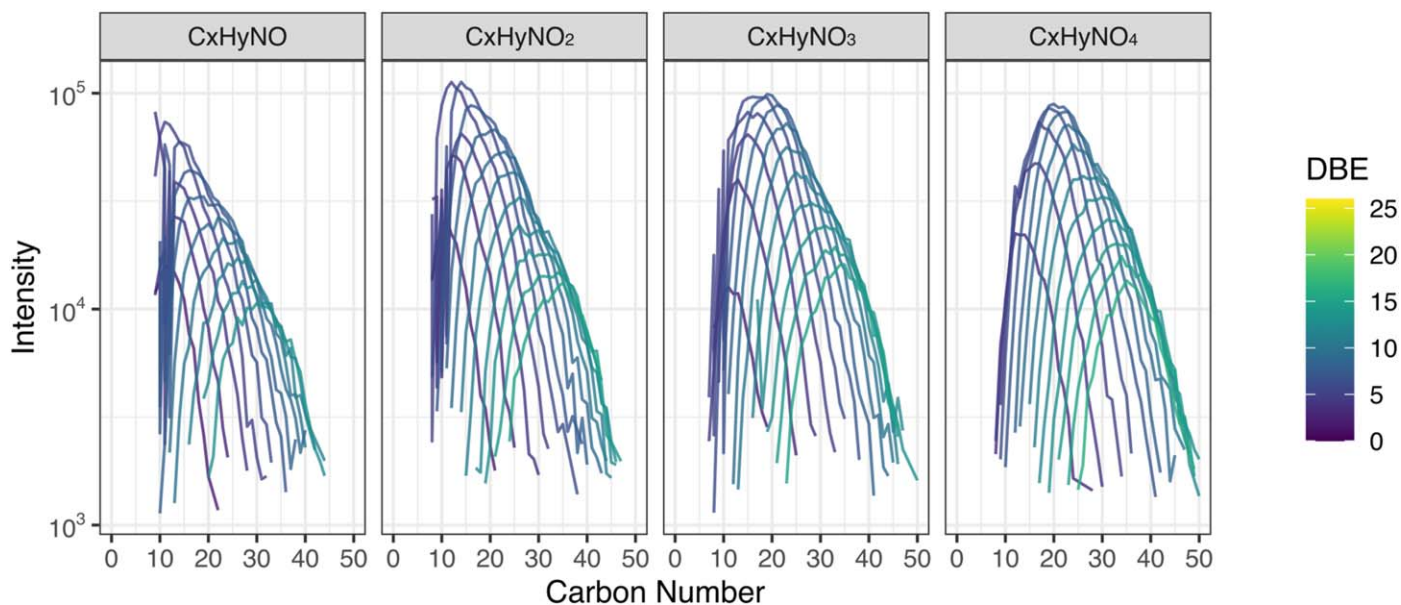


Figure A8. Modified mass spectra as a function of carbon number. The panels show the mass distributions of Nebulotron SOM (Zandanel 2021). We conducted SOM extraction and analyses in the same manner with the Tagish Lake meteorite (Isa et al. 2019). We define a CH₂ family, known as an alkyl homologous series, as all molecules that have the same stoichiometric formulae except for the number of repeating CH₂. They are treated similar to the alkyl homologous compounds that were identified in a previous study of the Murchison meteorite (Naraoka et al. 2017). Molecules bearing N(1) and O(1–4) were selected and organized by the number of O atoms. They are colored by DBE values.

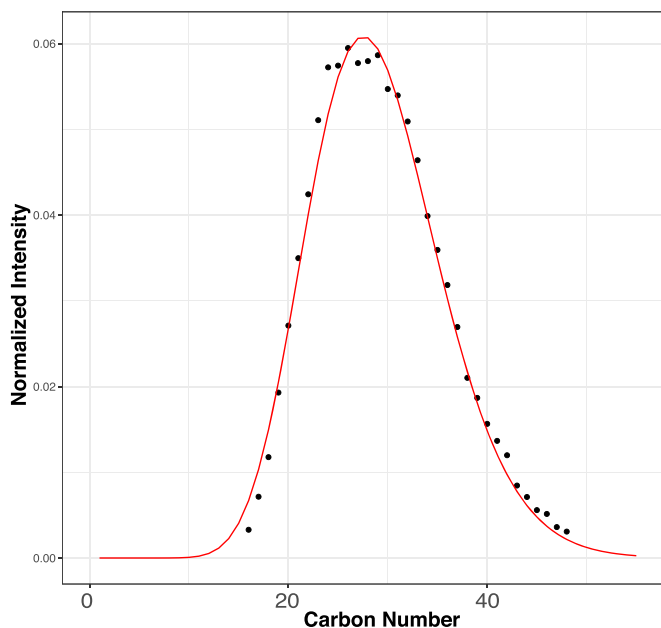


Figure A9. The SZ fit for the data of Nebulotron (the data are the same as Figure A8). An example CH₂ family, C₁₄H₉NO + (CH₂)_n, is selected.

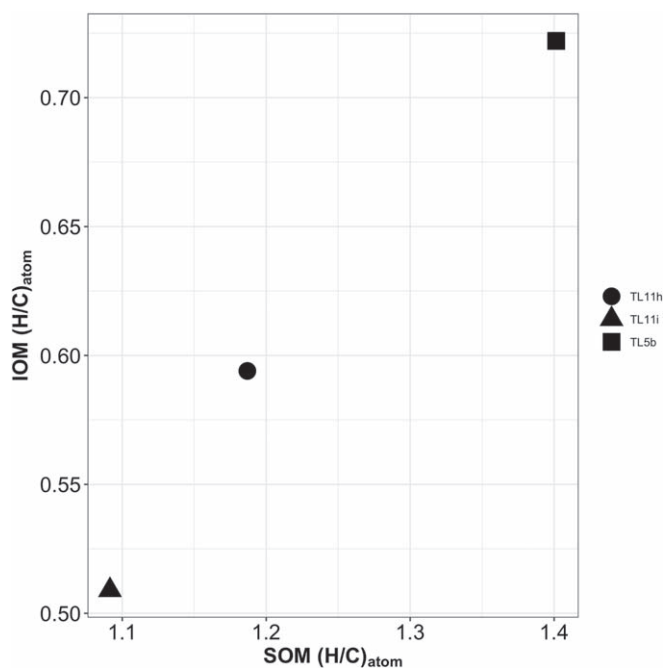


Figure A10. Atom H/C ratio of SOM vs. atom H/C ratio of IOM. The SOM H/C ratios were calculated by averaging over the N-bearing assigned ions' relative intensity. For the bulk SOM H/C ratio, which is the filled square in the figure, we used all of the assigned spectra. The IOM data are from a previous study (Alexander et al. 2014).

Appendix B Orbitrap Measurement Methods

The SOM extracted from the Tagish Lake meteorite powder was measured by the high-resolution mass spectra Thermo LTQ Orbitrap XL instrument coupled with an ESI source in the m/z^{-1} range of 150–800 at the University of Grenoble Alpes. The positive ions were analyzed with a resolving power of $m/\Delta m \sim 100,000$ at $m/z^{-1} = 400u$. For the analyses, the direct infusion technique was used. The SOM, together with the solvent, was injected continuously into the Orbitrap at a flow rate of $3 \mu\text{l minute}^{-1}$. The flow rate was controlled by the syringe pump attached to the instrument, and the PEEK capillary tube was used. One direct infusion analysis took approximately 30 minutes.


Appendix C Data Analyses

After we acquired the spectra, we utilized the postprocessing data analysis tools that have been developed in-house at IPAG. ATTRIBUTOR was used for the main data analyses, and the following data treatment was applied using an in-house code written in the R language. The postprocessing includes peak detection, noise rejection, and mass-drift correction. After we refined the mass spectra, we assigned the chemical formulae to the detected peaks. The chemical formulae were assigned using ^{12}C , ^{13}C , H, ^{14}N , and ^{16}O . The assigned chemical formulae were filtered based on the offset from the ideal mass calculated based on the assigned chemical formulae. The filter was ± 1.5 ppm. In this paper, we only used the chemical formulae assigned with ^{12}C .

We define a CH₂ family, known as an alkyl homologous series, as all molecules that have the same stoichiometric formulae except for the number of repeating CH₂. They are treated similar to the alkyl homologous compounds that were identified in a previous study of the Murchison meteorite (Naraoka et al. 2017).

ORCID iDs

Junko Isa  <https://orcid.org/0000-0001-9046-296X>

François-régis Orthous-Daunay  <https://orcid.org/0000-0002-1170-0550>

Pierre Beck  <https://orcid.org/0000-0002-6532-5602>

Christopher D. K. Herd  <https://orcid.org/0000-0001-5210-4002>

Veronique Vuitton  <https://orcid.org/0000-0001-7273-1898>

Laurène Flandinet  <https://orcid.org/0000-0001-7190-7396>

References

- Alexander, C. M. O. D., Cody, G. D., Kebukawa, Y., et al. 2014, *M&PS*, 49, 503
 Alexander, C. M. O. D., & Ebel, D. S. 2012, *M&PS*, 47, 1157

- Alexander, C. M. O. D., Fogel, M., Yabuta, H., & Cody, G. D. 2007, *GeCoA*, 71, 4380
 Alexander, C. M. O. D., Newsome, S. D., Fogel, M. L., et al. 2010, *GeCoA*, 74, 4417
 Alves, R. F., Casalini, T., Storti, G., & McKenna, T. F. 2021, *Macromol. React. Eng.*, 15, 2000059
 Bekaert, D. V., Derenne, S., Tissandier, L., et al. 2018, *ApJ*, 859, 142
 Blinova, A. I., Herd, C. D. K., & Duke, M. J. M. 2014b, *M&PS*, 49, 1100
 Blinova, A. I., Zega, T. J., Herd, C. D. K., & Stroud, R. M. 2014a, *M&PS*, 49, 473
 Braukmüller, N., Wombacher, F., Hezel, D. C., Escoube, R., & Münker, C. 2018, *GeCoA*, 239, 17
 Brown, P. G., Hildebrand, A. R., Zolensky, M. E., et al. 2000, *Sci*, 290, 320
 Cafferty, B. J., & Hud, N. V. 2014, *Curr Opin Chem Biol*, 22, 146
 Cody, G. D., & Alexander, C. M. O. D. 2005, *GeCoA*, 69, 1085
 Cody, G. D., Heying, E., Alexander, C. M. O. D., et al. 2011, *PNAS*, 108, 19171
 Förtsch, D., Pabst, K., & Groß-Hardt, E. 2015, *ChEnS*, 138, 333
 Friedrich, J. M., Wang, M. S., & Lipschutz, M. E. 2002, *M&PS*, 37, 677
 Furukawa, Y., Chikaraishi, Y., Ohkouchi, N., et al. 2019, *PNAS*, 116, 24440
 Gilmour, C. M., Herd, C. D. K., & Beck, P. 2019, *M&PS*, 54, 1951
 Glavin, D. P., & Dworkin, J. P. 2009, *PNAS*, 106, 5487
 Grady, I. M. M., Verchovsky, A. B., Franchi, A., Wright, P., & Pillinger, C. T. 2002, *M&PS*, 37, 713
 Grady, M. M., Graham, A. L., Barber, D. J., et al. 1987, *PolRe*, 46, 162
 Guo, W., & Eiler, J. M. 2007, *GeCoA*, 71, 5565
 Herd, C. D. K., Blinova, A., Simkus, D. N., et al. 2011, *Sci*, 80, 1304
 Hilt, R. W., Herd, C. D. K., Simkus, D. N., & Slater, G. F. 2014, *M&PS*, 49, 526
 Jones, R. H. 2012, *M&PS*, 47, 1176
 Kallemeyn, G. W., & Wasson, J. T. 1981, *GeCoA*, 45, 1217
 Koga, T., Parker, E. T., McLain, H. L., et al. 2021, *M&PS*, 56, 1005
 Kuga, M., Cernogora, G., Marrocchi, Y., Tissandier, L., & Marty, B. 2017, *GeCoA*, 217, 219
 Kuga, M., Marty, B., Marrocchi, Y., & Tissandier, L. 2015, *PNAS*, 112, 7129
 Mittlefehldt, D. W. 2002, *M&PS*, 37, 703
 Naraoka, H., & Hashiguchi, M. 2019, *GeocJ*, 53, 33
 Naraoka, H., Yamashita, Y., Yamaguchi, M., & Orthous-Daunay, F. R. 2017, *ESC*, 1, 540
 Oba, Y., & Naraoka, H. 2009, *M&PS*, 44, 943
 Orthous-Daunay, F. R., Piani, L., Flandinet, L., et al. 2019, *GeocJ*, 53, 21
 Pizzarello, S., Huang, Y., Becker, L., et al. 2001, *Sci*, 293, 2236
 Pladis, P., & Kiparissides, C. 1998, *ChEnS*, 53, 3315
 Quirico, E., Bonal, L., Beck, P., et al. 2018, *GeCoA*, 241, 17
 Schmitt-Kopplin, P., Gabelica, Z., Gougeon, R. D., et al. 2010, *PNAS*, 107, 2763
 Scholz, G. V. 1939, *ZPC*, 43, 25
 Simkus, D. N., Aponte, J. C., Elsila, J. E., et al. 2019, *PLSci*, 54, 1283
 Spaeth, A., & Hargrave, M. 2020, *Life*, 10, 12
 Suttle, M. D., King, A. J., Schofield, P. F., Bates, H., & Russell, S. S. 2021, *GeCoA*, 299, 219
 Urey, H. C., & Craig, M. 1953, *GeCoA*, 4, 36
 Warren, P. H. 2011, *E&PSL*, 311, 93
 Wasson, J. T., & Kallemeyn, G. W. K. 1988, *RSPTA*, 325, 535
 Wlotzka, F., Spettel, B., Palme, H., & Schultz, L. 1989, in 52nd Annual Meeting of the Meteoritical Society, Two New CM Chondrites from Antarctica: Different Mineralogy, But Same Chemistry, 52, 269
 Yabuta, H., Williams, L. B., Cody, G. D., Alexander, C. M. O. D., & Pizzarello, S. 2007, *M&PS*, 42, 37
 Zandanel, A. E. 2021, Doctoral dissertation, Univ. Grenoble Alpes
 Zimm, B. H. 1948, *JChPh*, 16, 1093
 Zolensky, M. E., Nakamura, K., Gounelle, M., et al. 2002, *M&PS*, 37, 737
 Zolotov, M. Y., Mironenko, M. V., & Shock, E. L. 2006, *M&PS*, 41, 1775